Current Topics

Cutting Edge Developments in RNA Biology for the Control of Gene Expression

Regular Article

BAY61-3606 Alters snRNP Composition and Enhances Usage of Suboptimal Splice Acceptor Site

Kenji Tomita,[a] Shinichi Nakagawa,[a,b] Hiroyoshi Ariga,[a,b] and Hiroshi Maita*[,a,b]

[a] *Graduate School of Life Sciences, Hokkaido University, Sapporo 060–0812, Japan: and* [b] *Faculty of Pharmaceutical Sciences, Hokkaido University, Sapporo 060–0812, Japan.*

Received June 30, 2022; accepted October 26, 2022

Intron recognition by the spliceosome mainly depends on conserved intronic sequences such as 5′ splice sites, 3′ splice sites, and branch sites. Therefore, even substitution of just a single nucleotide in a 5′ or 3′ splice site abolishes the splicing at the mutated site and leads to cryptic splice site usage. A number of disease-causative mutations have been found in 5′ and 3′ splice sites, but the genes with these mutations still maintain the correct protein-coding sequence, so recovery of splicing at the mutated splice site may produce a normal protein. Mutations in the spliceosome components have been shown to change the balance between the conformational transition and disassembly of the spliceosome, which affects the decision about whether the reaction of the incorporated substrate will proceed. In addition, the lower disassembly rate caused by such mutations induces splicing of the mutated splice site. We hypothesized that small compounds targeting the spliceosome may include a compound mimicking the effect of those mutations. Thus, we screened a small-compound library and identified a compound, BAY61-3606, that changed the cellular small nuclear ribonucleoprotein composition and also showed activity of enhancing splicing at the mutated 3′ splice site of the reporter gene, as well as splicing at the suboptimal 3′ splice site of endogenous cassette exons. These results indicate that further analysis of the mechanism of action of BAY61-3606 could enable modulation of the fidelity of splicing.

Key words splicing, split luciferase, small nuclear ribonucleoprotein, fidelity, small compound screening

INTRODUCTION

Pre-mRNA splicing is a reaction catalyzed by the spliceosome, which removes an intron followed by exon ligation to produce mature mRNA. The spliceosome is assembled on an intron by the deposition of a subcomplex called small nuclear ribonucleoprotein (snRNP) with extensive conformational changes. Five different snRNPs are required for spliceosome formation, each of which contains one of U1, U2, U4, U5, and U6 snRNA bound with specific proteins.[1–3] During spliceosome assembly on the substrate pre-mRNA, the intron region must be selected accurately to avoid the formation of aberrant transcripts.

Recognition of the intron by the spliceosome mainly depends on the conserved short nucleotide sequences called the 5′ splice site and the 3′ splice site, which are located at both ends of introns; most introns start with the sequence GU and end with AG. In addition to the 5′ and 3′ splice sites, the branch site sequence (BS) upstream of the 3′ splice site containing the adenine nucleotide forming the lariat structure also plays important roles. In addition, the pyrimidine stretch between the branch site and the 3′ splice site helps recognition of these splice sites. A mutation substituting only a single nucleotide of the 5′ or 3′ splice site almost completely abolishes splicing at the site and often induces splicing at a cryptic splice site, indicating the stringent fidelity of this process. Actually, many human disease-associated mutations have been found in four invariant nucleotides (positions: +1, +2, −1, −2) of the 5′ and 3′ splice sites,[4] but genes with those mutations still maintain the correct protein-coding sequence. Rescuing splicing defects is a potential therapeutic approach, although no strategies have yet been developed due to the lack of a sufficient understanding of the fidelity mechanism.

At the beginning of spliceosome assembly, U1 snRNP recognizes the 5′ splice site through base pairing interaction of U1 snRNA with that site. As for the BS and the 3′ splice site, following SF1 binding to the BS, the SF3B complex in the U2 snRNP interacts with the BS cooperating with the heterodimer of U2AF65 and U2AF35. U2AF65 and U2AF35 bind to the pyrimidine stretch and AG of the 3′ splice site, respectively. Subsequent conformational change of U2 snRNP including the release of SF1 is required to progress to the next step. Mutations of SF3B1, U2A35, and other related factors found in myelodysplastic syndrome[5] alter the preference of BS and the 3′ splice site.[6–9] Disease-causative mutations differently affect the function of mutated proteins, such as by altering the binding preference to the nucleotide or by affecting the protein–protein interaction[10–13]; however, the overall mechanism can be interpreted as the change of equilibrium of the conformational transition of U2 snRNP.

Even after the substrate sequence passes the recognition step described above, if the candidate sequence is mutated, several later steps can also abort the reaction to discard the aberrant substrate.[14] This rejection mechanism is carried out kinetically by balancing between the assembly and disassembly of the spliceosome. The assembly pathway of the spliceosome involves many ATPases to accelerate remodeling of the complex and their functional defects are often accompanied by increased splicing at the aberrant splice site.[15–20] Therefore,

* To whom correspondence should be addressed. e-mail: maimai@pharm.hokudai.ac.jp

these ATPases are thought to be bi-functional, acting not only for remodeling of the complex, but also for disassembly of the spliceosome to discard the aberrant substrate. It is inferred that impaired disassembly prolongs retention of the aberrant substrate in the spliceosome, resulting in proceeding to the next step of the splicing reaction. In addition to ATPase mutants, mutations in structural proteins such as Prp8, which surrounds the RNA core of the spliceosome, as well as a mutant of sky1p kinase, which phosphorylates the splicing factors, also decrease the fidelity of splice site recognition.[21–24] This means that factors affecting the stability of the spliceosome could change the balance between the conformational transition and the disassembly, resulting in alteration of the fidelity of splicing. Small compounds altering this balance would be able to modulate this fidelity. Spliceostatin A and pladienolide B, compounds targeting SF3B1, have been shown to alter the branch site selection,[25,26] but these compounds do not enhance the splicing at the mutated 3′ splice site.

Previously, we found that two flavones, luteolin and apigenin, have such activity to enhance the usage of the mutated 3′ splice site within a splicing reporter gene.[27] Recently, these compounds were also shown to be effective for genes containing disease-associated mutations.[28] However, the mechanism of action of luteolin on splicing remains unknown and generally flavones have a broad range of targets, so it is difficult to use flavones as tools for further analysis to elucidate the mechanism maintaining the fidelity of splicing.[29,30] Against this background, to identify novel small compounds that relax the fidelity of splicing, as the first screening, we used the split luciferase assay that detects the cellular snRNP levels,[31] instead of the splicing reporter,[27] which was expected to concentrate compounds directly targeting the spliceosome. Following second screening of the collection of compounds using the splicing reporter gene, the compound BAY61-3606 was identified. It altered the cellular snRNP composition and also enhanced the splicing at the mutated 3′ splice site in the reporter gene, as well as the inclusion of endogenous cassette exons with the weak 3′ splice site.

MATERIALS AND METHODS

Cell Culture and Reagents The 293T cell line and its derivative cell lines were cultured in Dulbecco's modified Eagle's medium (DMEM) with 10% fetal bovine serum. For transient reporter expression, cells were transfected with the reporter plasmids (Fig. 1) using Lipofectamine 2000 reagent (ThermoFisher, Waltham, MA, U.S.A.), in accordance with the manufacturer's instruction. To establish the 293T cell line stably expressing a reporter gene pair (pSplit-Osp-ON-Prp6 and pSplit-Myc-OC-Prp4), reporter plasmids and pRNA-H1-tet-Hygro, a plasmid coding hygromycin resistant gene, were co-transfected followed by selection for hygromycin B resistance. Small compounds used in this study (Supplementary Table 1) were purchased and the compound library was provided by the Drug Discovery Initiative of the University of Tokyo. Plasmid vectors of the split luciferase were already reported.[31] To make the stable transfectant of the reporter pair of Prp6 and Prp4, plasmids expressing the reporter proteins were modified to exchange the tag peptide from FLAG-tag to One-STrEP tag II and Myc-tag, respectively. A minigene reporter, pFD-Luc-Py-AT, for the splicing assay has already been reported.[27]

Split Luciferase Assay The cells expressing the split luciferase reporter were lysed in SL buffer [20 mM *N*-(2-hydroxyethyl)piperazine-*N*′-2-ethanesulfonic acid (HEPES)-KOH (pH 7.9), 150 mM NaCl, 1.5 mM $MgCl_2$, and 0.5% Triton X-100] supplemented with protease inhibitors (1 mM p-ABSF, 2 μg/mL leupeptin, 5 μg/mL pepstatin A, 10 μg/mL aprotinin). After centrifugation at 11100 $\times$ ***g*** for 1 min, an aliquot of the supernatant was mixed with 100 μL of luciferase substrate solution (Steady-Glo Luciferase Assay System; Promega, Madison, WI, U.S.A.), and luminescence was immediately detected using Lumat LB9507 (Berthold Technologies, Baden-Wurttemberg, Germany). To calibrate the transfection efficiency, pActin-β-gal, a plasmid encoding β-galactosidase, was co-transfected with the reporters. The β-galactosidase activity was measured as absorbance at 450 nm by reacting with ONPG and was used to correct the luciferase activity. For *in vitro* assay, reporter proteins were synthesized using TnT Coupled Reticulocyte Lysate Systems (Promega) in 30 μL and synthesized proteins were mixed at 2.5 μL each and incubated for 15 min on ice. The luciferase activities of these mixtures were immediately measured after addition of the luciferase substrate Steady-Glo.

Glycerol Gradient Analysis Whole-cell lysate prepared as described above was loaded onto 10–40% glycerol gradients in SL buffer. Samples were centrifuged in 11 mL gradients at 4 °C for 15 h at 37000 rpm in an SW41 rotor. Fractions were collected from the top of the gradient manually and aliquots (20 μL) were used to detect luminescence using Lumat LB9507 (Fig. 2). Proteins in the remaining half of a fraction were precipitated by adding 2 volumes of cold acetone and precipitates were suspended in 100 μL of Laemmli buffer for sodium dodecyl sulfate (SDS)-polyacrylamide gel electrophoresis (PAGE).

Western Blotting and Antibodies Proteins were separated on an 8 or 12% polyacrylamide gel and subjected to Western blotting with respective antibodies. Each antibody was further reacted with IRDye 800-conjugated secondary antibodies (Rockland, Philadelphia, PA, U.S.A.) or Alexa Fluor 680-conjugated secondary antibodies (Molecular Probes, Eugene, OR, U.S.A.) for visualization by an IR imaging system (Odyssey; LI-COR, Lincoln, NE, U.S.A.). The antibodies used were mouse monoclonal anti-DYKDDDDK (Wako Pure Chemical Corporation, Osaka, Japan), mouse monoclonal anti-Myc (9E10; Santa Cruz Biotechnology, Dallas, TX, U.S.A.), mouse monoclonal anti-Actin (c4; Merck/Millipore, Burlington, MA, U.S.A.), mouse monoclonal anti-Prp8 (2834c1a; Abcam, Cambridge, U.K.), mouse monoclonal anti-StrepTag II (71590; Novagen, U.S.A.), rabbit polyclonal anti-SART3 (A301-522A; Bethyl Laboratories, U.S.A.), rat monoclonal anti-Prp3 antibodies,[32] rat polyclonal anti-Prp6 serum, and rat monoclonal anti-Prp6. Rat anti-Prp6 antibodies were obtained by immunizing rats with recombinant human Prp6 (1–398 a.a.) in adjuvant and serum and lymph nodes were collected 2 weeks later. The cells from lymph nodes were fused to the mouse myeloma cell line X63/Ag8-653 and positive clones were selected. All animal experiments were carried out in accordance with the National Institutes of Health Guide for the Care and Use of Laboratory Animals, and the protocols were approved by the Committee for Animal Research at Hokkaido University (Permit No. 08-0468).

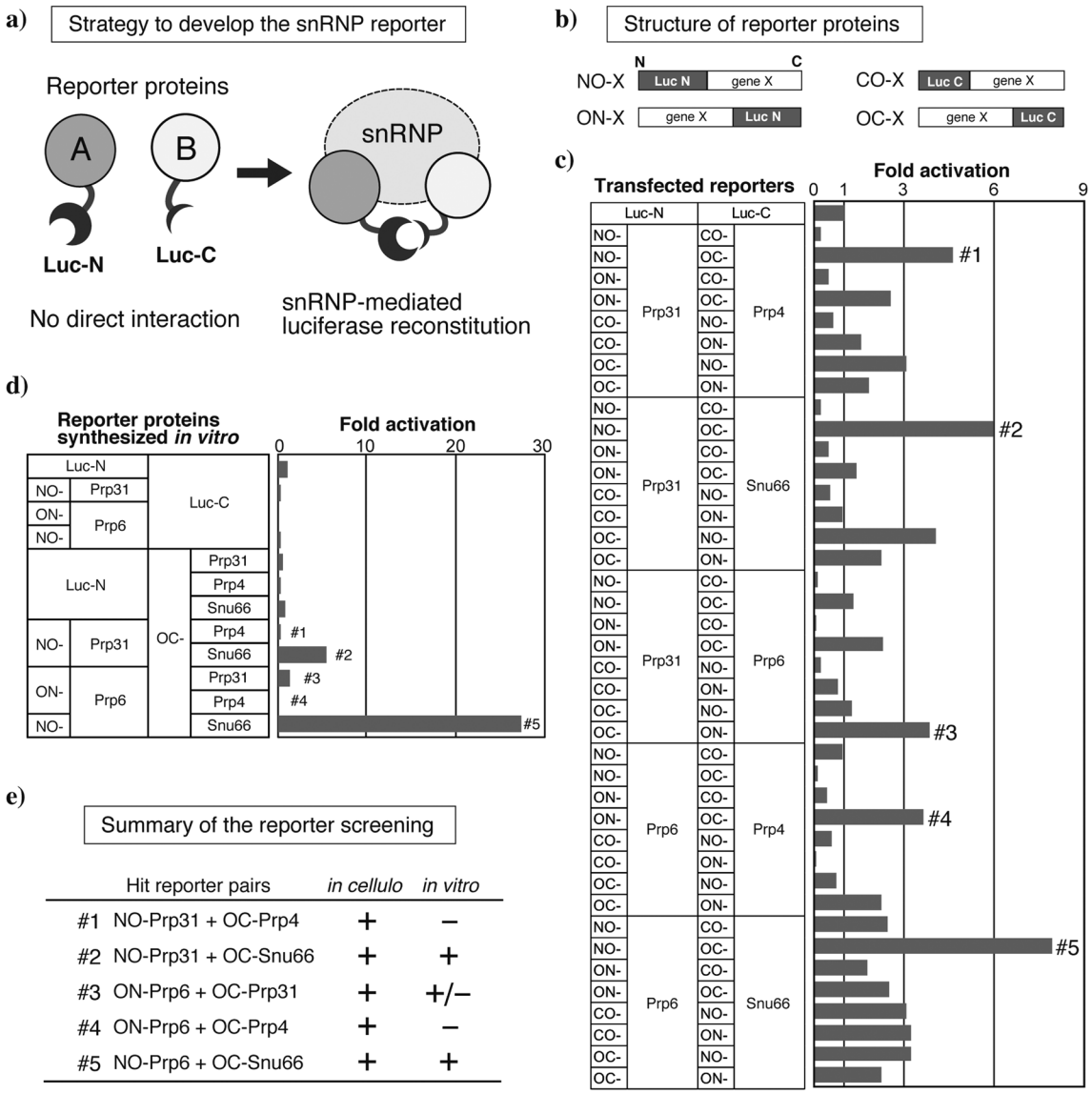

Fig. 1. Screening of Reporter Protein Pairs

(a) The working model of the split luciferase reporter to detect the cellular snRNP level. Expected reporter pairs that reconstitute the luciferase activity only within the snRNP. (b) Schematic structure of the luciferase fragment-fused proteins expressed from the reporter vector library. (c) Reconstituted luciferase activities of cells transiently transfected with reporter vector pairs as indicated in the left panel. Luciferase activities are presented as fold change relative to cells transfected with empty vectors. #1–5 indicate the reporter pairs that were further tested *in vitro*. (d) Reconstituted luciferase activities of reporter proteins synthesized *in vitro*. #1–5 on the right side of bars are the same as in (c). (e) Summary of screening of the reporter pairs. Reporter pairs with no luminescence *in vitro* are expected to behave as snRNP reporters.

Screening of Compound Library Detailed methods for the compound screening using a split luciferase reporter will be described elsewhere (*in preparation*). In brief, the day before the screening, approximately 6×10^4 293T reporter cells were seeded manually in white-wall 96-well plates. Library compounds were diluted to 20 μM with medium in other plates and half of the medium of the cell plates was replaced with medium containing compounds (final concentration: 10 μM) and the plates were incubated for 4 h at 37 °C. After incubation, cells were lysed in BN buffer [20 mM Hepes-KOH (pH 7.4), 2 M KCL, 0.5 M 6-aminohexanoic acid, 0.5% Triton-X100, 10% glycerol]. Lysed cells were mixed with the substrate solution (Steady-Glo; Promega) and the luminescence was measured using a multimode plate reader (EnSpire; PerkinElmer, Inc., Waltham, MA, U.S.A.). Hit compounds were obtained based on the fold change of luciferase activity compared with the average activity of surrounding wells as control and the compounds yielding over a 25% increase or decrease were considered as hit compounds (Fig. 3). Hit compounds were further tested twice in the same assay to confirm the reproducibility. To handle the large number of plates, we used Hornet-HTS (Wako Pure Chemical Corporation), a programmable automatic pipetting machine.

Minigene Reporter Assay The 293T cells were transfected with pFD-Luc-Py-AT in six-well plates and 24 h later small compounds were added to the culture. After incubation for another 24 h, cells were lysed in RNAiso (TaKaRa, Shiga, Japan) to extract total RNA for RT-PCR; alternatively, cells were lysed in SL buffer to measure the luciferase activity. To detect splicing isoforms by RT-PCR, RNAiso (TaKaRa) and ReverTra Ace RT Master Mix (TOYOBO, Osaka, Japan) were used for RNA extraction and reverse transcription, respectively. ExTaq (TaKaRa) was used for PCR. Primers were ex17-up (sense primer): 5′-

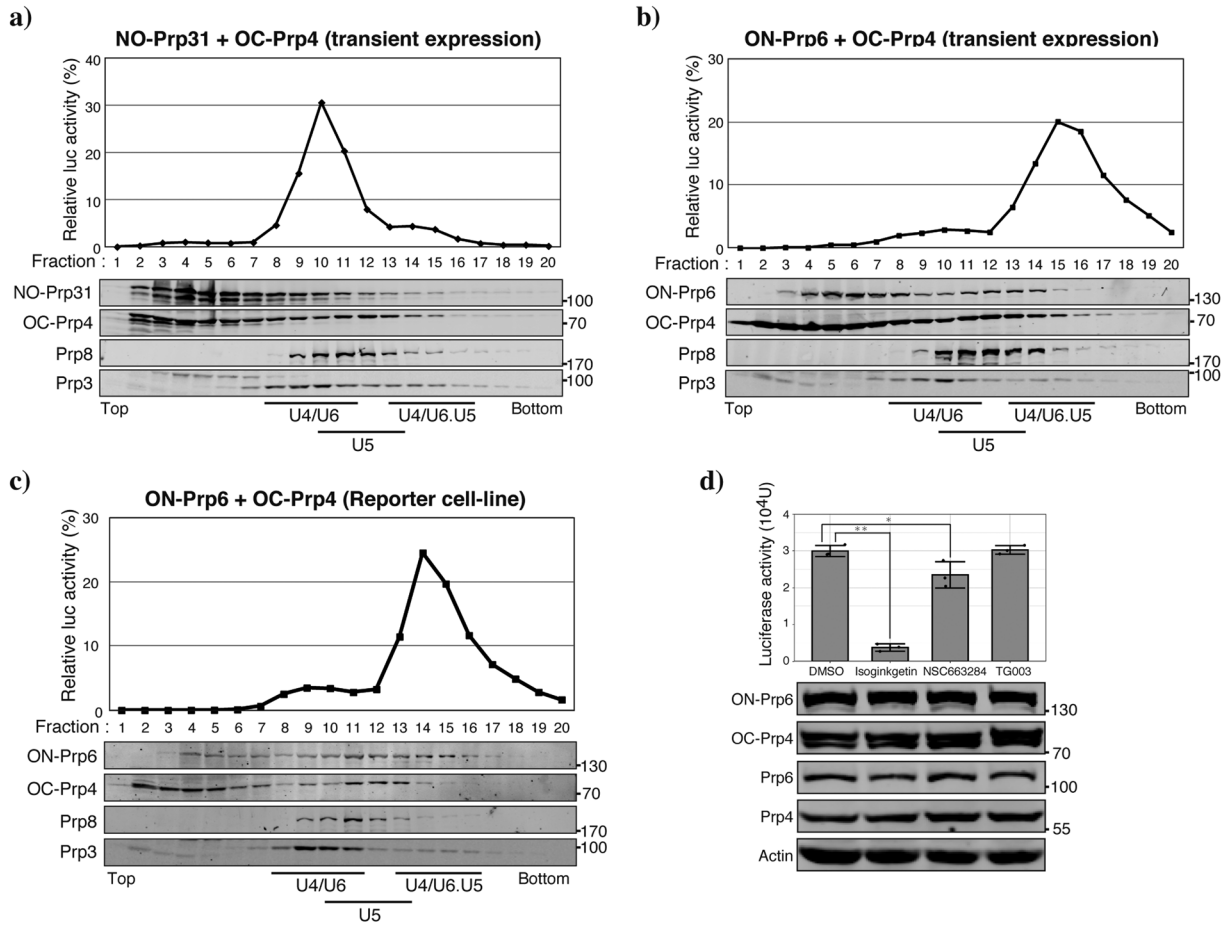

Fig. 2. Confirmation of Incorporation of the Reporter Activity into a Large Complex

Whole-cell lysates of reporter protein pairs, Prp31–Prp4 (a) and Prp6–Prp4 (b, c), were fractioned by 10–40% glycerol density gradient centrifugation. Experiments were performed by transient transfection (a, b) or stable introduction (c) of reporter vectors. Luciferase activity of each fraction was calculated as the proportion relative to the sum of luminescence of all fractions. Lower panels are of Western blotting of the reporter and marker proteins of snRNPs. (d) Response of the reporter cell line to compounds known to inhibit or modulate splicing. Mean luciferase activities of three independent experiments are presented as bars. Each set of data is plotted as dots and error bars indicating standard deviation (S.D.) (*$p<0.05$, **$p<0.01$, $n=3$, Bonferroni/Dunnett test). No differences in protein expression were observed for both reporter proteins and endogenous counterparts (lower panels).

GCTGTACAAGTCCGGACTC-3′ and pFD-as-IRD1 (labeled, antisense primer): 5′-GCCCAGCTTCACAGTAGTG-3′-IRD800. PCR products separated in 2% agarose were scanned and quantified using Odyssey (LI-COR). Because the upper band is produced by splicing at the noncanonical 3′ splice site,[27] the proportion of upper band intensity relative to the sum of the upper and lower bands was calculated for comparison. To detect splicing efficiency by the reporter activity, whole-cell lysate was transferred to a black-wall plate to measure GFP fluorescence using Glomax (Promega). Then, cell lysates were further transferred to a white-wall plate and luciferase substrate solution, Steady-Glo (Promega), was added to detect the luciferase activity using Glomax. After subtraction of the average counts of empty wells as a background signal, relative luciferase activity was calculated as the ratio of the luciferase luminescence to GFP fluorescence. To test the dose response, a stable transfectant of 293T cells with pFD-Luc-Py-AT was used. The cell line was selected by hygromycin resistance after co-transfection with pFD-Luc-Py-AT and pRNA-H1-tet-Hygro.

IP-RT-qPCR Antibodies used for immunoprecipitation were absorbed on Protein A/G PLUS-Agarose (Santa Cruz Biotechnology) in advance and the buffer was exchanged to SL buffer. Cells in a 10 cm dish treated for 4 h with a small compound were lysed in SL buffer, followed by centrifugation at 11100 × ***g***, after which the supernatant was collected. Antibodies on beads were reacted with the supernatant by rotating for 1 h at 4 °C. After extensive washing with SL buffer, RNA was extracted using RNAiso and 2 μL (one-fifth) of the purified RNA from the 10 cm dish was used as a template for reaction in a 10 μL volume at RT. ReverTra Ace qPCR RT kit (TOYOBO) and SYBR Premix Ex Taq II (TaKaRa) were used in line with the manufacturers' instructions for reverse transcription and qPCR, respectively. Quantitative PCR was carried out using MiniOpticon (Bio-Rad, Hercules, CA, U.S.A.). The relative amount of snRNA in the precipitate was calculated using input snRNA as a standard (Fig. 4). Primers used were as follows. Reverse primers were also used for reverse transcription.

U4 snRNA Forward: 5′-GCGCGATTATTGCTAATTGAAA-3′
U4 snRNA Reverse: 5′-AAAAATTGCCAATGCCGACTA-3′
U5 snRNA Forward: 5′-GGTTTCTCTTCAGATCGCATAAATC-3′
U5 snRNA Reverse: 5′-CTCAAAAAATTGGGTTAAGACTCAGA-3′
U6 snRNA Forward: 5′-GCTTCGGCAGCACATATACTAAAAT-3′
U6 snRNA Reverse: 5′-ACGAATTTGCGTGTCATCCTT-3′

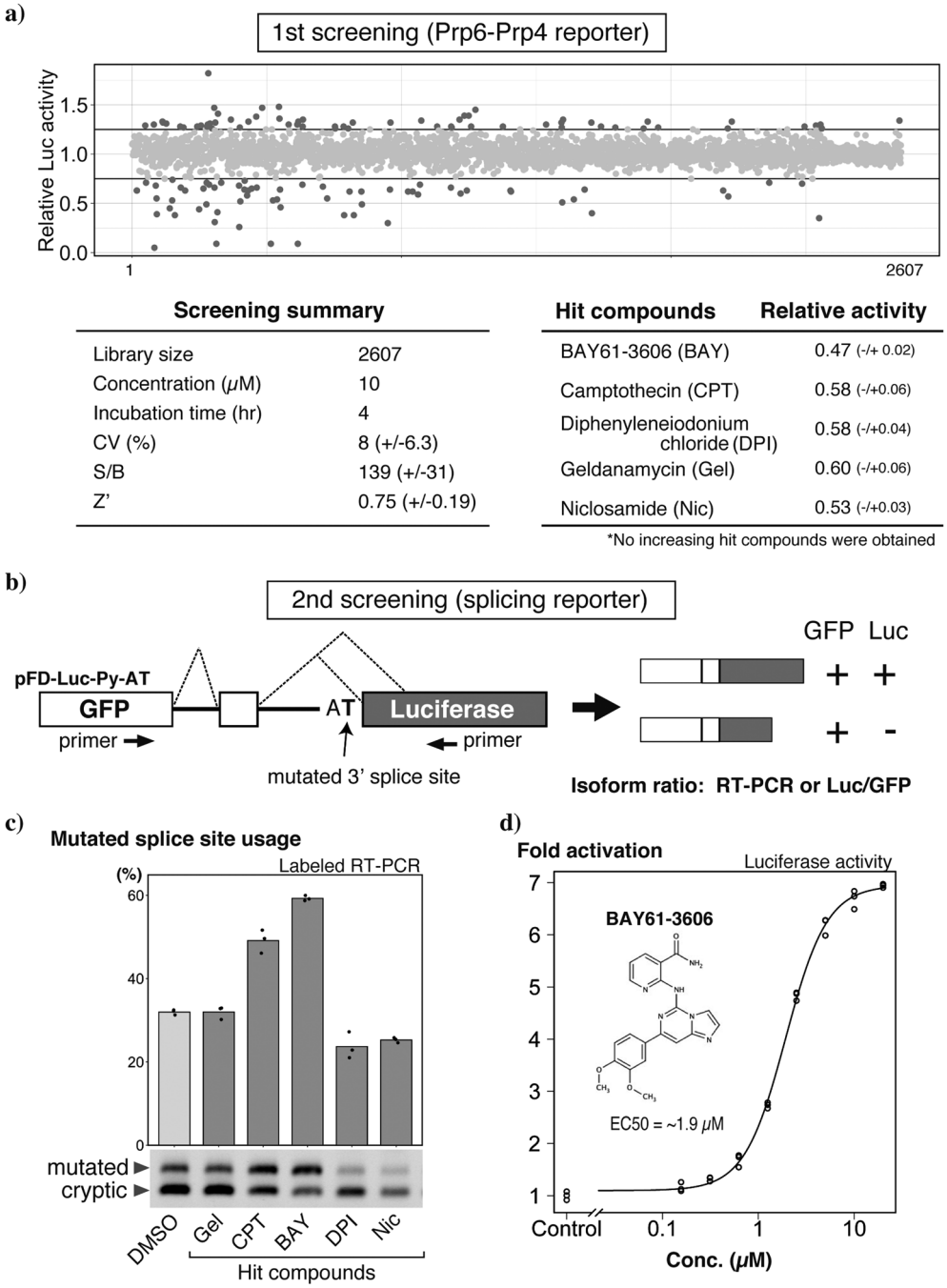

Fig. 3. (a) Fold Change of the Reconstituted Luciferase Activity after 4 h of Treatment of Library Compounds at 10 μM Is Indicated as Dots

(b) Schematic of the minigene splicing reporter. The 3′ splice site of the second intron is mutated from AG to AT. This mutation leads to downstream cryptic splice site usage, as indicated by dotted lines. Reporter protein translated from the isoform from the cryptic site lacks luciferase activity while retaining GFP fluorescence, allowing detection of the efficiency of the splicing at the mutated 3′ splice site by both RT-PCR and luciferase activity corrected by GFP fluorescence. (c) The results of the second screening using the minigene splicing reporter. Lower panel is a representative gel image; bands were obtained by RT-PCR using the labeled primer. The upper band is the isoform from the mutated 3′ splice site. Bars show the mean proportion of upper bands relative to total spliced transcripts from three technical replicates. Raw values of technical replicates are overlaid as dots. (c) EC_{50} of BAY61-3606's splicing modulatory activity was calculated from the dose-response curve. Splicing change was detected by the luciferase activity corrected by GFP fluorescence. Dots indicate values from two independent experiments and each value is the mean of three technical replicates.

Splicing Analysis of Whole Transcriptome Total RNA extracted from 293T cells treated with dimethyl sulfoxide (DMSO) or BAY61-3606 for 4 h was used for library preparation for RNA-seq using a Ribo-zero Gold ribosomal RNA (rRNA) Removal Kit (Illumina, San Diego, CA, U.S.A.) and TruSeq RNA Sample Preparation v2 (Illumina), in accordance with the manufacturer's instructions. Single-end sequencing reads obtained by HiSeq2500 (Illumina) were mapped to hg38 by STAR (ver. 2.5.3a).[33] The resulting Bam files were used as input for rMATS (ver. 3.2.5).[34–36] Values of the inclusion level difference from significantly altered splicing isoforms were used to make boxplots, as shown in Fig. 5a. To compare the splice site scores, the required lengths of sequences around the splice site for MaxEnt analysis were obtained using bedtools based on the bed files of the cassette, upstream and downstream exons that were separated into four groups by combining with data on the response to BAY61-3606, and the direction of splicing change. Obtained fasta files were used

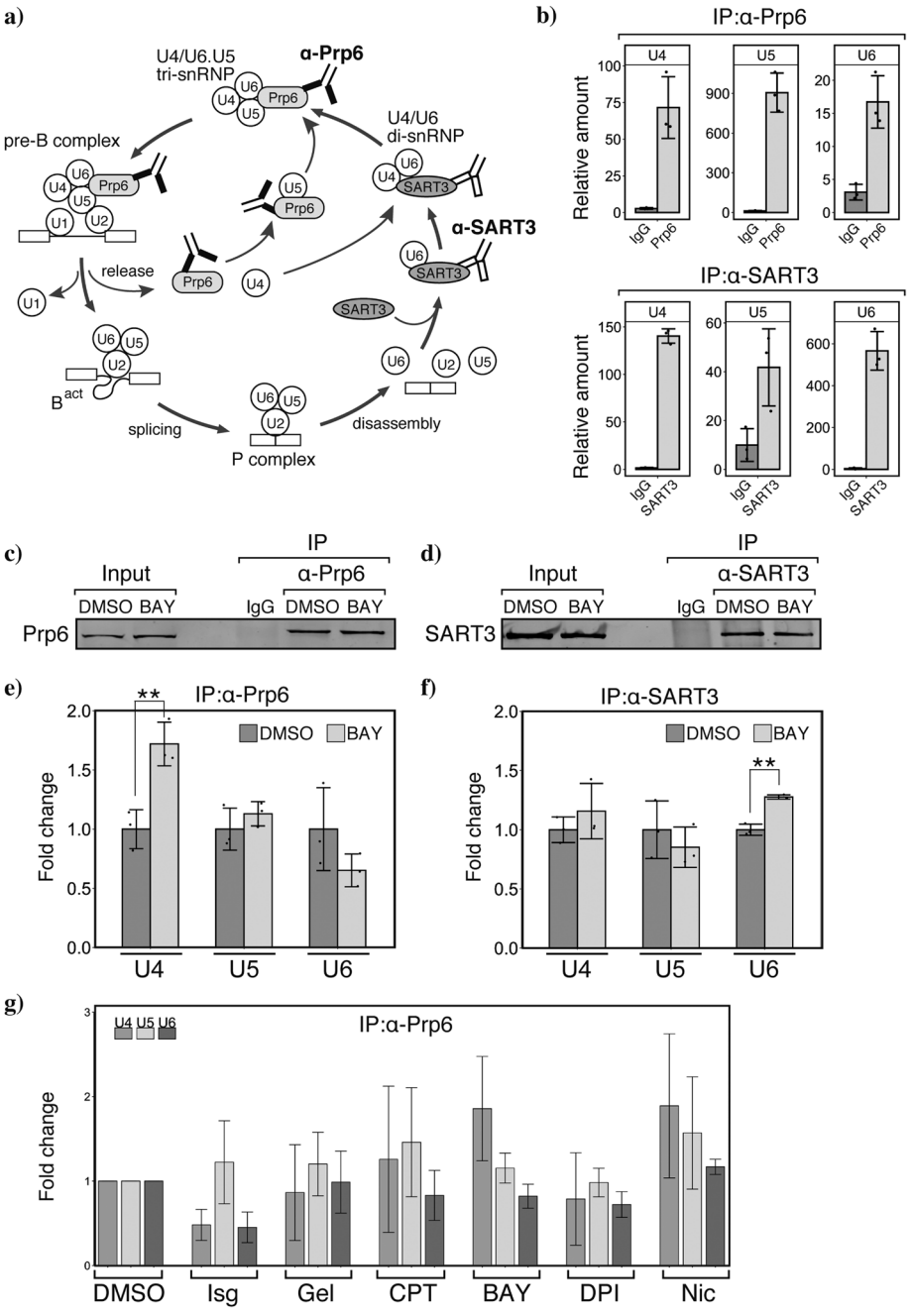

Fig. 4. (a) Schematic Model of the Spliceosome Assembly Pathway

Antibodies against Prp6 and SATR3 are shown as "Y" shapes to indicate which complexes are captured by each antibody. (b) RT-qPCR of U4, U5, and U6 snRNA in the immunoprecipitates by Prp6 or SART3 antibodies. Normal IgG was used as a control. Bars and dots represent mean and each count of three independent experiments. Error bars indicate S.D. ($n = 3$). (c) Western blotting confirming immunoprecipitation of Prp6 and SART3 antibodies both in the presence and in the absence of BAY61-3606. (e, f) Comparison of U4, U5, and U6 snRNA levels in the immunoprecipitates by Prp6 or SART3 antibodies in the presence of BAY61-3606. Bars and dots represent mean and each count of three independent experiments. Error bars indicate S.D. (** $p < 0.01$, $n = 3$, Student's t-test). (g) Comparison of U4, U5, and U6 snRNA levels in the immunoprecipitates by Prp6 antibodies in the presence of compounds decreasing the Prp6–Prp4 snRNP reporter activity. Bars represent mean of three independent experiments. Error bars indicate S.D. ($n = 3$).

as input for MaxEnt analysis[37] (http://hollywood.mit.edu/burgelab/maxent/Xmaxentscan_scoreseq.html) and the result files containing splice site scores were plotted using R.

Statistics Quantified data shown in Figs. 2 and 4 were obtained from three independent experiments. Amount of snRNA recovered by immunoprecipitation was normalized using the standard curve prepared by using diluted total RNA. In addition, to compare changes of U4, U5, and U6 snRNA on a uniform basis, relative amount of recovered snRNA was normalized by the average of DMSO-treated samples. For statistical analysis, Bonferroni/Dunnett test was used as shown in Fig. 2d for multiple comparisons among multiple samples and Student's t-test was used in Fig. 4e. The significance of differences of predicted scores for splice sites affected by BAY61-3606 was analyzed by Wilcoxon rank sum test with Bonferroni correction.

RESULTS

Previously, we developed two types of genetic reporter to

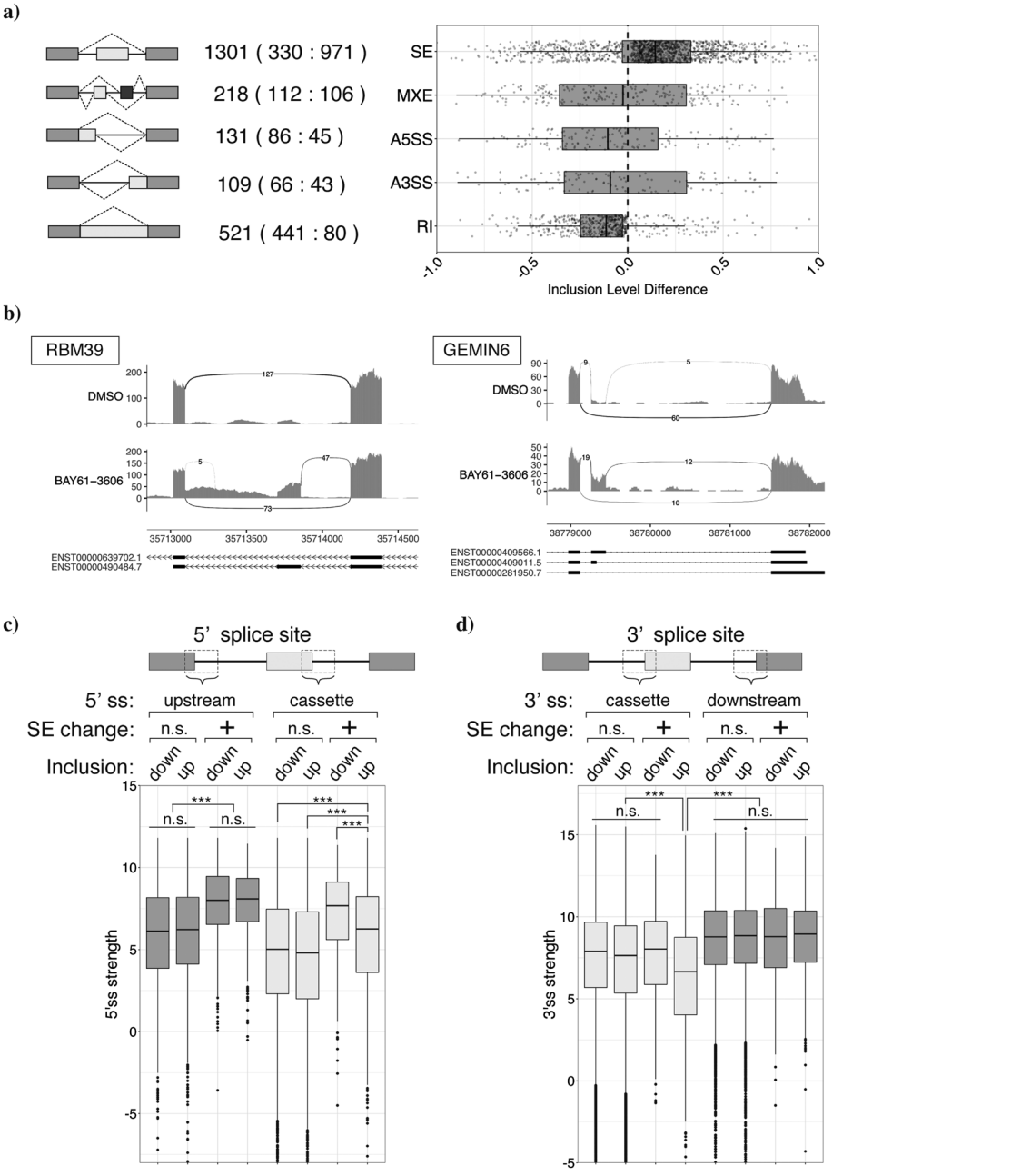

Fig. 5. (a) Summary of BAY61-3606-Induced Alternative Splicing (AS)

AS patterns are classified into five types as indicated on the left (SE: skipped exon, MXE: mutually exclusive exon, A5SS: alternative 5′ss usage, A3SS: alternative 3′ss usage, RI: retained intron). Isoforms produced by each AS were divided into two types with the labels p1: upper isoforms and p2: lower isoforms. The middle table shows which isoforms (p1 or p2) increased significantly. The right panel shows the distribution of significant AS events as a box plot. The x-axis indicates the levels of AS change between DMSO and BAY61-3606 treatment (maximum = 1.0) and all events are overlaid as dots. (c) Sashimi plot of representative BAY61-3606-induced alternative splicing. (d) Predicted scores of the 5′ and 3′ splice site signals calculated by MaxEnt are indicated as box plots. Splice site sequences were grouped by their responses to BAY61-3606 treatment and the direction of splicing change (inclusion down: p1 was increased, inclusion up: p2 was increased). Events without significant change were also grouped similarly. ***$p < 0.001$ by Wilcoxon rank sum test with Bonferroni correction.

test the activities of compounds related to the spliceosome. One is a minigene reporter containing a mutation in the 3′ splice site, which allows measurement of the activity inducing splicing at the mutated splice site.[27] Using this reporter, we manually screened a small set of compounds, which resulted in the identification of flavones such as luteolin and apigenin as compounds that relax the fidelity of 3′ splice site selection. However, flavones are not suitable for use as tools for studying the fidelity mechanism of splicing because they have many biological effects *via* various target proteins.[29] Meanwhile, we also developed the split luciferase reporter, which reflects the cellular U5 snRNP level.[31] This reporter was successfully applied to compound library screening in an automated manner (*in preparation*). Next, we planned to screen a larger compound library first using this split luciferase reporter, which would establish a collection of compounds that potentially target the spliceosome. In addition, the second screening of the collection using the minigene reporter could lead to the identification of compounds that alter the fidelity of splice site selection *via* the spliceosome.

Towards this aim, we attempted to develop a novel type of snRNP reporter because our previous reporter is specific

to free U5 snRNP, which is located far from spliceosome assembly. Thus, the compounds selected by this reporter are not necessarily related to the fidelity of splice site selection, which may cause a lower hit rate. We assumed that, if a reporter detecting more complex snRNPs on the path to spliceosome assembly, such as U4/U6.U5 tri-snRNP or precatalytic B complex ("pre-B complex" in Fig. 4a), were applied, it would be more suitable for compound screening to identify small molecules that modulate the fidelity of splicing.

To find such reporter protein pairs that reconstitute the luciferase activity within a larger snRNP complex like tri-snRNP, we prepared a reporter protein library consisting of core components of tri-snRNP that were expected to ensure the efficient incorporation of the reporter protein into tri-snRNP. We screened this reporter protein library by the luciferase activity of the cells that were transiently transfected with pairs of reporter vectors, as indicated in Fig. 1b. On the basis of the luciferase activity, five sets of reporter vectors were selected and subjected to further testing of whether the reporter proteins synthesized *in vitro* also reconstitute the luciferase activity without adding any other components, which could rule out the possibility that the reporter proteins reconstitute the luciferase activity by their direct interaction. As shown in Figs. 1c and d, gene pairs of Prp31–Prp4 and Prp6–Prp4 showed no luciferase activity by the synthesized proteins, suggesting that they only reconstitute the luciferase in the cellular environment, hopefully within the snRNP.

Next, we attempted to determine the size of the cellular complexes involving Prp31–Prp4 and Prp6–Prp4 reporter proteins. We performed glycerol gradient sedimentation analysis using whole-cell lysates from the cells transiently transfected with these reporters. As expected, both reporters showed luciferase activity in the heavier fractions, whereas reporter proteins were mostly detected in the lighter fractions (Figs. 2a, b). Notably, the positions of the peak fraction of the luciferase activity from these two reporter pairs differed. The Prp31–Prp4 pair showed the peak fraction at fraction#10, which overlapped with the peak fraction of Prp8 and Prp3 proteins used as markers of U5 and U4/U6 snRNP, respectively. In addition, a small peak was also seen between fractions#14 and#15. In contrast, the Prp6–Prp4 pair showed the main peak at fraction#15 and a small peak at fraction#10 (Figs. 2a, b). These differences suggest that the Prp6–Prp4 reporter activity mostly reflects U4/U6.U5 tri-snRNP or the larger complex including tri-snRNP, while the Prp31–Prp4 reporter activity would reflect the U4/U6 or U5 snRNPs. Thus, we established a stable cell line expressing the Prp6–Prp4 reporter proteins for compound screening. The established cell line was also examined by gradient analysis (Fig. 2c), which further clarified whether the reporter complex contained other snRNP proteins by immunoprecipitation of the reporter proteins (data not shown). Before applying the reporter to the compound screening, we tested whether the reporter activity is responsible for the small-compound-mediated perturbation of splicing. The reporter cells were treated with isoginkgetin, NSC663284, and TG003, which were reported to affect splicing, and the supernatant of whole-cell lysate was used to detect the luciferase activity.[38–40] As shown below the histogram, no compounds altered the expression levels of the reporter proteins and their endogenous counterpart; however, isoginkgetin significantly reduced the luciferase activity and NSC663284 slightly reduced it. Because isoginkgetin has been shown to prevent precatalytic B complex formation by reducing tri-snRNP,[39,41] the significant reduction of Prp6–Prp4 reporter activity is in agreement with the reporter complex reflecting the amount of tri-snRNP. Even if this were not the case, the reporter showed high responsiveness to the perturbation of spliceosome assembly, so we concluded that our reporter is suitable for compound screening.

Theoretically, our reporter can detect both increases and decreases of reporter activity, but our screening of 2607 compounds acquired only compounds that decreased the reporter activity. Five compounds remained after three rounds of reproducibility testing and their activities were also confirmed by commercially available compounds. We also tested whether there is a compound that affects the splicing fidelity using the minigene reporter. As shown in Fig. 3b, RT-PCR-based detection of splicing change of the reporter gene showed that camptothecin and BAY61-3606 exerted activity to increase splicing at the mutated 3′ splice site. In addition, such splicing modulatory activity of BAY61-3606 was not detected for the wild-type reporter (data not shown). Because BAY61-3606 showed a stronger effect and is known as a multiple kinase inhibitor specific for Syk kinase[42] as well as several MAP kinases and cyclin-dependent kinases,[43] we were interested in the mechanism by which BAY61-3606 affects splicing. Other Syk kinase inhibitors did not show any activity on splicing similar to BAY61-3606 (data not shown), so we concluded that the target of BAY61-3606 related to splicing is not Syk kinase. First, to determine the effective concentration and EC_{50} of BAY61-3606 in the splicing assay, dose response was examined. As splicing change of the minigene reporter can be detected by the isoform-specific production of luciferase, we made a stable cell line expressing the minigene reporter to detect the splicing change by the luciferase activity. Using this splicing reporter cell line, BAY61-3606 was shown to be highly effective over 5 μM, as shown in Fig. 3b.

Because BAY61-3606 was identified by the split luciferase reporter that detects changes of the cellular snRNP level, we next tested whether BAY61-3606 truly affected endogenous snRNP levels. Towards this aim, we employed an approach of detecting snRNA by RT-qPCR from immunopurified snRNP particles. Although many antibodies against snRNP proteins were not suitable to precipitate snRNAs (data not shown), our newly developed anti-Prp6 monoclonal antibody and commercially available anti-SART3 antibody specifically precipitate corresponding snRNAs (Fig. 4b). Prp6 is a constitutive component of U5 snRNP, so it is predicted to bind U5 snRNP as well as the U4/U6.U5 tri-snRNP and the precatalytic B complex. Based on Prp6 being released during the conversion of precatalytic B complex to the Bact complex, the complexes expected in the particles immunopurified by Prp6 antibody are indicated in the cartoon (Fig. 4a). As expected, Prp6 antibody highly accumulated U5 snRNA compared with U4 and U6 (Fig. 4b). In addition, the efficiency of co-precipitation of U4 snRNA with Prp6 was slightly higher than that of U6 snRNA. As U4 snRNA is released from the precatalytic B complex at a similar timing to Prp6, the difference of positions of each snRNA in the spliceosome may cause the difference of co-precipitation efficiency. SART3 is a recycling factor of U6 snRNA that assists the re-annealing of U6 snRNA with U4 snRNA *via* binding free U6 snRNA after

splicing catalysis,[44,45] so it strongly interacts with U6 snRNP and U4/U6 snRNP. Indeed, in the particles immunopurified by the SART3 antibody, U6 snRNA was the most abundant and U5 snRNA was present at a much lower level than U4 and U6 snRNA (Fig. 4b). Next, we tested whether BAY61-3606 alters the snRNA composition. First, total levels of snRNA in the presence or absence of BAY61-3606 were detected by Northern blotting and RT-qPCR (Supplementary Fig. 1). Interestingly, RT-qPCR showed that expression of U5 snRNA was increased up to 1.5-fold in the presence of BAY61-3606, although it was not clear in Northern blotting. Then, we compared the abundance of snRNA in the antibody-purified particles and found that co-precipitation of U4 snRNA with the Prp6 antibody was significantly increased in the presence of BAY61-3606. No such significant changes were found in other conditions (Figs. 4e, f). Furthermore, as shown in Supplementary Fig. 2, in the condition where Prp8 was knocked down and both tri-snRNP and U5 snRNP were reduced, ON-Prp6 and OC-Prp4 reporter proteins showed luciferase activity outside of the original distribution, suggesting the formation of an aberrant complex involving both reporter proteins. However, in the case of BAY61-3606 treatment, the luciferase activity was decreased but the peak position was not changed (Supplementary Fig. 3). This suggests that the increased Prp6-U4 snRNA complex may not contain Prp4 and the normal tri-snRNP involving both Prp6 and Prp4 was decreased. In addition, we further tested whether other hit compounds also show similar activity in the same experiment using Prp6 antibody. Strikingly, isoginkgetin showed reductions of U4 and U6 snRNA compared with U5 snRNA and the pattern clearly differed from that of BAY61-3606. This isoginkgetin-induced reduction of tri-snRNP was shown in a previous study,[41] validating our method. Other compounds also showed some slight trends of change, but we have not tested them further.

BAY61-3606 has been suggested to modulate the snRNP composition by an unknown mechanism and this perturbation may be related to increased splicing at the mutated 3′ splice site of the minigene reporter. Thus, we became interested in its effect on splicing of the whole transcriptome and performed RNA-seq analysis of cells treated with BAY61-3606. Triplicate RNA samples for both DMSO and BAY61-3606 treatment were prepared and mapped sequence reads were analyzed by rMATS, a program to detect the splicing pattern changes.[34–36] As shown in Fig. 5a, alternative splicing was classified into five classes in this program. Each alternative splicing event produces two mutually exclusive isoforms, as indicated in the schematic image (Fig. 5a left columns). The total number of significant changes of alternative splicing detected by rMATS is about 2300 events; half of those are changes of exon skipping. In addition, BAY61-3606 mainly increased the inclusion of cassette exons and representative changes of exon inclusion are presented in Fig. 5b. A decrease of retained introns was also found in the presence of BAY61-3606. To investigate which type of cassette exons were upregulated for inclusion, both 5′ and 3′ splice site sequences were collected and the scores predicted by the MaxEnt algorithm[37] were plotted (Figs. 5c, d). Comparison of the predicted scores clearly indicates two characteristic features of the splice sites of the BAY61-3606-responsive cassette exons. The 5′ splice site of the BAY61-3606-responsive cassette exons showed significantly better scores than the non-responsive cassette exons, which was also true for the 5′ splice site of the upstream exons. Interestingly, the 5′ splice site of the cassette exons of increased inclusions by BAY61-3606 showed weaker scores than other 5′ splice sites of the upstream exons or the cassette exons showing BAY61-3606-responsive decreased inclusions. In addition to the 5′ splice site, the 3′ splice site also showed a significant feature. Cassette exons that responded to BAY61-3606 contain a significantly weaker 3′ splice site than all other 3′ splice sites. These characteristic features indicate that the BAY61-3606-responsive cassette exons are normally skipped by their weakness of the 3′ splice site and, if the 3′ splice site recognition is shifted to a more sensitive state to detect the suboptimal site, those exons can be included, which may be related to the results obtained by the minigene reporter assay.

DISCUSSION

Here, we showed the results of our screening to identify a novel splicing-modulating compound. Although the spliceosome is recognized as a potential target for novel therapeutics to various diseases,[46–49] small compounds that modulate the spliceosome are still limited. The group of compounds that is growing the most is natural products targeting SF3B1.[49–51] These compounds affect splicing *via* interfering with the conformational transition of U2 snRNP required for entering into the precatalytic B complex, which results in massive change of splicing patterns *in vivo*. This is thus expected to counteract abnormally proliferating cells in cancer and MDS containing mutations in splicing factors.[46,49] However, if the aim of using splicing modulators is to restore aberrant splicing, compounds with a milder effect on the spliceosome are required. Therefore, we attempted to develop an assay aimed at collecting compounds that have weaker activities on the spliceosome, which partially alter the splicing pattern rather than inhibiting splicing altogether.

Although the principle of using a split luciferase-based reporter to detect the cellular snRNP levels was already reported in our previous study,[31] here we extended the application to other snRNP complexes and showed that the developed Prp6–Prp4 reporter was able to respond to known splicing modulators. Although it remains unclear which assembly intermediate of the spliceosome is detected by this reporter, the response of the Prp6–Prp4 reporter to isoginkgetin suggests that the luciferase activity is related to tri-snRNP because isoginkgetin has been shown to reduce tri-snRNP.[41] In addition, when U5 snRNP was reduced by Prp8 knockdown, the reporter showed a different peak of the luciferase activity in the lighter fraction (Supplementary Fig. 2b), suggesting that if both reporter proteins can be involved in the intermediate complex in the appropriate conformation, the reporter can reconstitute the luciferase activity. In contrast, although BAY61-3606 decreased Prp6–Prp4 reporter activity similarly to isoginkgetin, it decreased only U4 snRNA in the immunopurified Prp6 particles, suggesting that the modes of action of these two compounds differ. Sedimentation analysis of the split luciferase activity (Supplementary Fig. 3) showed that BAY61-3606 just leads to a reduction of the luciferase activity in peak fractions, without a change of distribution, suggesting that Prp6 particle containing U4 snRNA may not contain Prp4.

As for the mechanism of action of BAY61-3606, although it

increased co-precipitation of U4 snRNA in the Prp6–antibody particles, there is no complex consisting of U5 snRNP and U4 snRNA. One possible explanation of this observation is the delayed release of Prp6 and U4 snRNP. At this activation step of the spliceosome, large compositional and structural changes occur and the step is considered as a commitment for determining the splice site to use. This transition step has been shown to be regulated by post-translational modifications such as phosphorylation of Prp31 and Prp6 by PRP4 kinase.[52] Since BAY61-3606 is a multiple kinase inhibitor, it is possible that inhibition of phosphorylation including these proteins causes the delayed release of Prp6 and U4 snRNP, which may result in the increase of their interaction. Alternatively, treatment of BAY61-3606 may simply induce formation of the aberrant complex of Prp6 and U4 snRNA, which is not formed in the normal assembly pathway of the spliceosome. This is shown in cases with the addition of a dominant negative Prp28 mutant[53] or a small compound cp028.[54] A similar phenomenon could have been triggered by the kinase-inhibitory activity of BAY61-3606. Clearly more studies are required to elucidate the mechanism by which BAY61-3606 affects snRNPs.

Our analysis showed that, in the presence of BAY61-3606, the mutated 3′ splice site in the minigene reporter as well as cassette exons with a weaker 3′ splice site was more efficiently spliced than in the control condition, which suggests that BAY61-3606-mediated snRNP modulation relaxes the fidelity of the 3′ splice site selection. Interestingly, the cassette exons that responded to BAY61-3606 have better 5′ splice sites than the non-responsive cassette exons, which means that the mechanism of exon skipping of these cassette exons under normal conditions depends on the weakness of the 3′ splice site. GO analysis of genes with these cassette exons revealed that splicing factors were the second largest group of genes with enrichment. It is thus possible that the 3′ splice sites of these cassette exons may be evolutionarily adapted to autonomously regulate splicing factors by sensing the condition of the spliceosome.

Our study shows the possibility of obtaining small compounds that modulate the fidelity of splicing *via* targeting the spliceosome, which may lead to a strategy for recovering splicing at mutated 3′ splice sites. However, further studies are needed to elucidate the detailed mechanisms by which BAY61-3606 alters splicing.

Acknowledgments We thank Rie Nakaido, Yumi Komatsu, and the staff of the Center for Research and Education on Drug Discovery, Hokkaido University, for their assistance. We also thank Rei Yoshimoto for valuable discussion. This study was supported by JSPS KAKENHI Grant Numbers 21790056, 23790068, and 20K07028 to H.M. and Toray Science and Technology Grant and JSPS KAKENHI Grant Number 17H03604 to S.N. This study was also supported by JSPS KAKENHI Grant Number 16H06279 (PAGS) and Platform Project for Supporting Drug Discovery and Life Science Research [Basis for Supporting Innovative Drug Discovery and Life Science Research (BINDS)] from AMED under Grant Number JP21am0101001.

Conflict of Interest The authors declare no conflict of interest.

Supplementary Materials This article contains supplementary materials.

REFERENCES

1) Wahl MC, Will CL, Lührmann R. The spliceosome: design principles of a dynamic RNP machine. *Cell*, **136**, 701–718 (2009).
2) Will CL, Lührmann R. Spliceosome structure and function. *Cold Spring Harb. Perspect. Biol.*, **3**, a003707 (2011).
3) Wilkinson ME, Charenton C, Nagai K. RNA splicing by the spliceosome. *Annu. Rev. Biochem.*, **89**, 359–388 (2020).
4) Anna A, Monika G. Splicing mutations in human genetic disorders: examples, detection, and confirmation. *J. Appl. Genet.*, **59**, 253–268 (2018).
5) Yoshida K, Ogawa S. Splicing factor mutations and cancer. *Wiley Interdiscip. Rev. RNA*, **5**, 445–459 (2014).
6) DeBoever C, Ghia EM, Shepard PJ, Rassenti L, Barrett CL, Jepsen K, Jamieson CHM, Carson D, Kipps TJ, Frazer KA. Transcriptome sequencing reveals potential mechanism of cryptic 3′ splice site selection in SF3B1-mutated cancers. *PLOS Comput. Biol.*, **11**, e1004105 (2015).
7) Darman RB, Seiler M, Agrawal AA, *et al.* Cancer-associated SF3B1 hotspot mutations induce cryptic 3′ splice site selection through use of a different branch point. *Cell Reports*, **13**, 1033–1045 (2015).
8) Okeyo-Owuor T, White BS, Chatrikhi R, Mohan DR, Kim S, Griffith M, Ding L, Ketkar-Kulkarni S, Hundal J, Laird KM, Kielkopf CL, Ley TJ, Walter MJ, Graubert TA. U2AF1 mutations alter sequence specificity of pre-mRNA binding and splicing. *Leukemia*, **29**, 909–917 (2015).
9) Shirai CL, Ley JN, White BS, Kim S, Tibbitts J, Shao J, Ndonwi M, Wadugu B, Duncavage EJ, Okeyo-Owuor T, Liu T, Griffith M, McGrath S, Magrini V, Fulton RS, Fronick C, O'Laughlin M, Graubert TA, Walter MJ. Mutant U2AF1 expression alters hematopoiesis and pre-mRNA splicing *in vivo*. *Cancer Cell*, **27**, 631–643 (2015).
10) Tang Q, Rodriguez-Santiago S, Wang J, Pu J, Yuste A, Gupta V, Moldón A, Xu Y-Z, Query CC. SF3B1/Hsh155 HEAT motif mutations affect interaction with the spliceosomal ATPase Prp5, resulting in altered branch site selectivity in pre-mRNA splicing. *Genes Dev.*, **30**, 2710–2723 (2016).
11) Jenkins JL, Kielkopf CL. Splicing factor mutations in myelodysplasias: insights from spliceosome structures. *Trends Genet.*, **33**, 336–348 (2017).
12) Zhang J, Ali AM, Lieu YK, Liu Z, Gao J, Rabadan R, Raza A, Mukherjee S, Manley JL. Disease-causing mutations in SF3B1 alter splicing by disrupting interaction with SUGP1. *Mol. Cell*, **76**, 82–95.e7 (2019).
13) Kataoka N, Matsumoto E, Masaki S. Mechanistic insights of aberrant splicing with splicing factor mutations found in myelodysplastic syndromes. *Int. J. Mol. Sci.*, **22**, 7789 (2021).
14) Semlow DR, Staley JP. Staying on message: ensuring fidelity in pre-mRNA splicing. *Trends Biochem. Sci.*, **37**, 263–273 (2012).
15) Burgess S, Couto JR, Guthrie C. A putative ATP binding protein influences the fidelity of branchpoint recognition in yeast splicing. *Cell*, **60**, 705–717 (1990).
16) Burgess SM, Guthrie C. A mechanism to enhance mRNA splicing fidelity: the RNA-dependent ATPase Prp16 governs usage of a discard pathway for aberrant lariat intermediates. *Cell*, **73**, 1377–1391 (1993).
17) Mayas RM, Maita H, Staley JP. Exon ligation is proofread by the DExD/H-box ATPase Prp22p. *Nat. Struct. Mol. Biol.*, **13**, 482–490 (2006).
18) Xu Y-Z, Query CC. Competition between the ATPase Prp5 and branch region-U2 snRNA pairing modulates the fidelity of spliceosome assembly. *Mol. Cell*, **28**, 838–849 (2007).
19) Koodathingal P, Novak T, Piccirilli JA, Staley JP. The DEAH box ATPases Prp16 and Prp43 cooperate to proofread 5′ splice site

cleavage during pre-mRNA splicing. *Mol. Cell*, **39**, 385–395 (2010).
20) Yang F, Wang X-Y, Zhang Z-M, Pu J, Fan Y-J, Zhou J, Query CC, Xu Y-Z. Splicing proofreading at 5′ splice sites by ATPase Prp28p. *Nucleic Acids Res.*, **41**, 4660–4670 (2013).
21) Umen JG, Guthrie C. Mutagenesis of the yeast gene PRP8 reveals domains governing the specificity and fidelity of 3′ splice site selection. *Genetics*, **143**, 723–739 (1996).
22) Dagher SF, Fu XD. Evidence for a role of Sky1p-mediated phosphorylation in 3′ splice site recognition involving both Prp8 and Prp17/Slu4. *RNA*, **7**, 1284–1297 (2001).
23) Query CC, Konarska MM. Suppression of multiple substrate mutations by spliceosomal prp8 alleles suggests functional correlations with ribosomal ambiguity mutants. *Mol. Cell*, **14**, 343–354 (2004).
24) Mayerle M, Raghavan M, Ledoux S, Price A, Stepankiw N, Hadjivassiliou H, Moehle EA, Mendoza SD, Pleiss JA, Guthrie C, Abelson J. Structural toggle in the RNaseH domain of Prp8 helps balance splicing fidelity and catalytic efficiency. *Proc. Natl. Acad. Sci. U.S.A.*, **114**, 4739–4744 (2017).
25) Corrionero A, Miñana B, Valcárcel J. Reduced fidelity of branch point recognition and alternative splicing induced by the anti-tumor drug spliceostatin A. *Genes Dev.*, **25**, 445–459 (2011).
26) Vigevani L, Gohr A, Webb T, Irimia M, Valcárcel J. Molecular basis of differential 3′ splice site sensitivity to anti-tumor drugs targeting U2 snRNP. *Nat. Commun.*, **8**, 2100 (2017).
27) Chiba M, Ariga H, Maita H. A splicing reporter tuned to non-AG acceptor sites reveals that luteolin enhances the recognition of non-canonical acceptor sites. *Chem. Biol. Drug Des.*, **87**, 275–282 (2016).
28) Banning A, Tikkanen R. Towards splicing therapy for lysosomal storage disorders: methylxanthines and luteolin ameliorate splicing defects in aspartylglucosaminuria and classic late infantile neuronal ceroid lipofuscinosis. *Cells*, **10**, 2813 (2021).
29) Arango D, Morohashi K, Yilmaz A, Kuramochi K, Parihar A, Brahimaj B, Grotewold E, Doseff AI. Molecular basis for the action of a dietary flavonoid revealed by the comprehensive identification of apigenin human targets. *Proc. Natl. Acad. Sci. U.S.A.*, **110**, E2153–E2162 (2013).
30) Kashyap D, Sharma A, Tuli HS, Sak K, Garg VK, Buttar HS, Setzer WN, Sethi G. Apigenin: a natural bioactive flavone-type molecule with promising therapeutic function. *J. Funct. Foods*, **48**, 457–471 (2018).
31) Maita H, Tomita K, Ariga H. A split luciferase-based reporter for detection of a cellular macromolecular complex. *Anal. Biochem.*, **452**, 1–9 (2014).
32) Maita H, Kitaura H, Ariga H, Iguchi-Ariga SMM. Association of PAP-1 and Prp3p, the products of causative genes of dominant retinitis pigmentosa, in the tri-snRNP complex. *Exp. Cell Res.*, **302**, 61–68 (2005).
33) Dobin A, Davis CA, Schlesinger F, Drenkow J, Zaleski C, Jha S, Batut P, Chaisson M, Gingeras TR. STAR: ultrafast universal RNA-seq aligner. *Bioinformatics*, **29**, 15–21 (2013).
34) Shen S, Park JW, Huang J, Dittmar KA, Lu Z-X, Zhou Q, Carstens RP, Xing Y. MATS: a Bayesian framework for flexible detection of differential alternative splicing from RNA-Seq data. *Nucleic Acids Res.*, **40**, e61 (2012).
35) Park JW, Tokheim C, Shen S, Xing Y. Identifying differential alternative splicing events from RNA sequencing data using RNASeq-MATS. *Methods Mol. Biol.*, **1038**, 171–179 (2013).
36) Shen S, Park JW, Lu Z-X, Lin L, Henry MD, Wu YN, Zhou Q, Xing Y. rMATS: robust and flexible detection of differential alternative splicing from replicate RNA-Seq data. *Proc. Natl. Acad. Sci. U.S.A.*, **111**, E5593–E5601 (2014).
37) Yeo G, Burge CB. Maximum entropy modeling of short sequence motifs with applications to RNA splicing signals. *J. Comput. Biol.*, **11**, 377–394 (2004).
38) Muraki M, Ohkawara B, Hosoya T, Onogi H, Koizumi J, Koizumi T, Sumi K, Yomoda J-I, Murray MV, Kimura H, Furuichi K, Shibuya H, Krainer AR, Suzuki M, Hagiwara M. Manipulation of alternative splicing by a newly developed inhibitor of Clks. *J. Biol. Chem.*, **279**, 24246–24254 (2004).
39) O'Brien K, Matlin AJ, Lowell AM, Moore MJ. The biflavonoid isoginkgetin is a general inhibitor of Pre-mRNA splicing. *J. Biol. Chem.*, **283**, 33147–33154 (2008).
40) Berg MG, Wan L, Younis I, Diem MD, Soo M, Wang C, Dreyfuss G. A quantitative high-throughput *in vitro* splicing assay identifies inhibitors of spliceosome catalysis. *Mol. Cell. Biol.*, **32**, 1271–1283 (2012).
41) Huranová M, Ivani I, Benda A, Poser I, Brody Y, Hof M, Shav-Tal Y, Neugebauer KM, Stanek D. The differential interaction of snRNPs with pre-mRNA reveals splicing kinetics in living cells. *J. Cell Biol.*, **191**, 75–86 (2010).
42) Yamamoto N, Takeshita K, Shichijo M, Kokubo T, Sato M, Nakashima K, Ishimori M, Nagai H, Li YF, Yura T, Bacon KB. The orally available spleen tyrosine kinase inhibitor 2-[7-(3, 4-dimethoxyphenyl)-imidazo [1, 2-c] pyrimidin-5-ylamino] nicotinamide dihydrochloride (BAY 61-3606) blocks antigen-induced airway inflammation in rodents. *J. Pharmacol. Exp. Ther.*, **306**, 1174–1181 (2003).
43) Lau KS, Zhang T, Kendall KR, Lauffenburger D, Gray NS, Haigis KM. BAY61-3606 affects the viability of colon cancer cells in a genotype-directed manner. *PLoS ONE*, **7**, e41343 (2012).
44) Raghunathan PL, Guthrie C. A spliceosomal recycling factor that reanneals U4 and U6 small nuclear ribonucleoprotein particles. *Science*, **279**, 857–860 (1998).
45) Bell M, Schreiner S, Damianov A, Reddy R, Bindereif A. p110, a novel human U6 snRNP protein and U4/U6 snRNP recycling factor. *EMBO J.*, **21**, 2724–2735 (2002).
46) Effenberger KA, Urabe VK, Jurica MS. Modulating splicing with small molecular inhibitors of the spliceosome. *Wiley Interdiscip. Rev. RNA*, **8**, 1381 (2017).
47) DeNicola AB, Tang Y. Therapeutic approaches to treat human spliceosomal diseases. *Curr. Opin. Biotechnol.*, **60**, 72–81 (2019).
48) Lu B, Abdel-Wahab O. Promoting spliceosome assembly for therapeutic intent. *Trends Pharmacol. Sci.*, **42**, 981–983 (2021).
49) Schneider-Poetsch T, Chhipi-Shrestha JK, Yoshida M. Splicing modulators: on the way from nature to clinic. *J. Antibiot* (Tokyo)., **74**, 603–616 (2021).
50) Kaida D, Motoyoshi H, Tashiro E, Nojima T, Hagiwara M, Ishigami K, Watanabe H, Kitahara T, Yoshida T, Nakajima H, Tani T, Horinouchi S, Yoshida M. Spliceostatin A targets SF3b and inhibits both splicing and nuclear retention of pre-mRNA. *Nat. Chem. Biol.*, **3**, 576–583 (2007).
51) Kotake Y, Sagane K, Owa T, Mimori-Kiyosue Y, Shimizu H, Uesugi M, Ishihama Y, Iwata M, Mizui Y. Splicing factor SF3b as a target of the antitumor natural product pladienolide. *Nat. Chem. Biol.*, **3**, 570–575 (2007).
52) Schneider M, Hsiao H-H, Will CL, Giet R, Urlaub H, Lührmann R. Human PRP4 kinase is required for stable tri-snRNP association during spliceosomal B complex formation. *Nat. Struct. Mol. Biol.*, **17**, 216–221 (2010).
53) Boesler C, Rigo N, Anokhina MM, Tauchert MJ, Agafonov DE, Kastner B, Urlaub H, Ficner R, Will CL, Lührmann R. A spliceosome intermediate with loosely associated tri-snRNP accumulates in the absence of Prp28 ATPase activity. *Nat. Commun.*, **7**, 11997 (2016).
54) Sidarovich A, Will CL, Anokhina MM, Ceballos J, Sievers S, Agafonov DE, Samatov T, Bao P, Kastner B, Urlaub H, Waldmann H, Lührmann R. Identification of a small molecule inhibitor that stalls splicing at an early step of spliceosome activation. *eLife*, **6**, e23533 (2017).